AIAA JOURNAL
Vol. 47, No. 1, January 2009

# Detection of the Crack in Cantilever Structures Using Fuzzy Gaussian Inference Technique

Harish C. Das*
*Institute of Technical Education and Research, Bhubaneswar, Orissa 751 010, India*
and
Dayal R. Parhi†
*National Institute of Technology, Rourkela, Orissa 769 008, India*

DOI: 10.2514/1.35927

**Detection of the cracks in beam structures using the fuzzy Gaussian inference technique has been investigated in this paper. The fuzzy-logic controller used in the present investigation consists of six input parameters and two output parameters. The input parameters to the fuzzy controller are the relative divergence of the first three natural frequencies and first three mode shapes in dimensionless forms. The output parameters of the fuzzy controller are the relative crack depth and relative crack location in dimensionless forms. To derive the fuzzy rules for the controller, theoretical expressions have been developed considering four parameters such as natural frequencies, mode shapes, crack depths, and crack locations. The strain-energy release rate has been used for calculating the local stiffnesses of the beam for a mode-I type of the crack. Several boundary conditions are outlined that take into account the crack location. Required fuzzy rules are derived for the fuzzy Gaussian controller. The experimental setup has been fabricated in the laboratory for verifying the robustness of the developed fuzzy controller. The developed fuzzy controller can predict the location and depth of the crack in close proximity with the real results.**

## Nomenclature

$A$ = cross-sectional area of the beam
$A_i$ = unknown coefficients of matrix $A$ ($i = 1$ to 12)
$a_1$ = depth of the crack
$B$ = width of the beam
$B_1$ = vector of exciting motion
$C_u$ = $(E/\rho)^{1/2}$
$C_y$ = $(EI/\mu)^{1/2}$
$E$ = Young's modulus of elasticity of the beam material
$F_i$ = experimentally determined function ($i = 1, 2$)
$i, j$ = variables
$J$ = strain-energy release rate
$K_{ij}$ = local flexibility matrix elements
$\bar{K}_u$ = $\omega L/C_u$
$\bar{K}_y$ = $(\omega L^2/C_y)^{1/2}$
$K_{1,i}$ = stress-intensity factors for $P_i$ loads ($i = 1, 2$)
$L$ = length of the beam
$L_1$ = location (length) of the crack from fixed end
$M_i$ = compliance constant ($i = 1, 4$)
$P_i$ = axial force ($i = 1$), bending moment ($i = 2$)
$Q$ = stiffness matrix for free vibration
$Q_1$ = stiffness matrix for forced vibration
$u_i$ = normal functions (longitudinal) $u_i(x)$ ($i = 1, 2$)
$V$ = aggregate (union)
$W$ = depth of the beam
$x$ = coordinate of the beam
$Y_0$ = amplitude of the exciting vibration
$y$ = coordinate of the beam
$y_i$ = normal functions (transverse) $y_i(x)$ ($i = 1, 2$)
$\beta$ = relative crack location ($L_1/L$)
$\Lambda$ = minimum operation
$\mu$ = $A\rho$
$\xi_1$ = relative crack depth ($a_1/W$)
$\rho$ = mass density of the beam
$\omega$ = natural circular frequency

Received 30 November 2007; revision received 27 August 2008; accepted for publication 30 September 2008. 

*Department of Mechanical Engineering; harishdas1965@gmail.com.
†Department of Mechanical Engineering; dayalparhi@yahoo.com.

## I. Introduction

SCIENTISTS and engineers throughout the world have been doing intensive research for fault diagnosis of cracked beams for the last several years. It is observed that stiffness of the beam undergoes variation due to the presence of a crack. This in turn affects the natural frequencies and mode shapes of the vibrating beam. The deviations of natural frequencies and mode shapes mainly depend on the location and intensity of the crack. The investigations reported in this paper are given next.

A combined analytical and experimental study has been conducted to develop efficient and effective damage-detection techniques for beam-type structures [1]. The uniform load surface (ULS) has been employed in this study due to its lower sensitivity to ambient noise. In combination with the ULS, two new damage-detection algorithms [i.e., the generalized fractal dimension (GFD) and simplified gapped-smoothing (SGS) methods] have been proposed. Both methods are then applied to the ULS of the cracked and delaminated beams obtained analytically, from which the damage location and size are determined successfully. Based on the experimentally measured curvature mode shapes, both the GFD and SGS methods are further applied to detect three different types of damage in carbon/epoxy composite beams. The method of the crack localization and sizing in a beam can be obtained from free and forced response measurements [2]. This method has been illustrated through numerical examples. The predictions for the crack location and size are in agreement when taking the noise and measurement error into account. The local effect of softening at the crack location can be simulated by an equivalent spring connecting the two segments of the beam [3]. The model uses the transfer matrix method in conjunction with the Bernoulli–Euler theories of beam vibration, modal analysis, and the fracture-mechanics principle to derive a characteristic equation that relates the natural frequencies. The proposed approach is verified by simulation results.

Damage detection in vibrating beams or beam systems has been done by discussing the amount of frequencies necessary to locate and quantify the damage uniquely [4]. Two different procedures of damage identification are used, which mainly take advantage of the

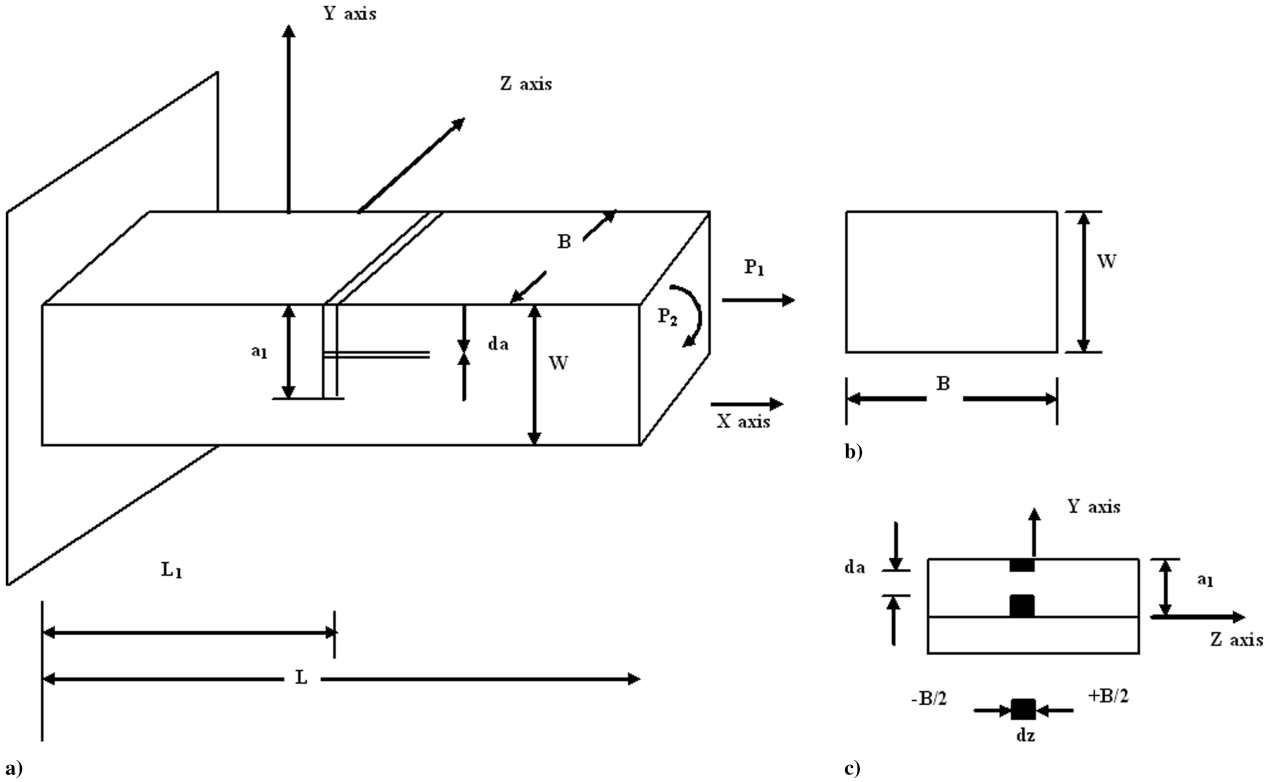


**Fig. 1 Segments taken during integration at the crack section: a) cantilever beam and b) cross-sectional view of the beam.**

peculiar characteristics of the problem. Cases with pseudoexperimental and experimental frequencies are solved. A crack has been simulated by an equivalent spring connecting the two segments of the beam [5]. Analysis of this approximate model results in algebraic equations that relate the natural frequencies to beam and crack characteristics. These expressions are then applied to studying the inverse problem identification of the crack location from frequency measurements. It is found that the only information required for accurate crack identification is the variation of the first two natural frequencies due to the crack, with no other information needed concerning the beam geometry or material and the crack depth or shape. The proposed method is confirmed by comparing it with results of numerical finite element calculations. The least-squares identification method, Kalman filtering method, and adaptive filtering method have been adopted to diagnose structural fault [6].

Equation of motion and corresponding boundary conditions has been developed for forced bending-vibration analysis of a beam with an open edge crack [7,8]. A uniform Euler–Bernoulli beam and the Hamilton principle have been used in this research. The crack has been modeled as a continuous-disturbance function in the displacement field that is obtained from fracture mechanics. Behzad et al. [7,8] have stated that there is an agreement between the theoretical results and those obtained by the finite element method. The natural frequencies have been obtained for bending vibrations of Timoshenko cracked beams with simple boundary conditions [9]. The beam is modeled as two segments connected by two massless springs (one extensional and another one rotational). This model promotes discontinuities in both vertical displacement and rotation due to bending, which are proportional to the shear force and bending moment transmitted by the cracked section, respectively. Loya et al.'s [9] results show that their method provides simple expressions for the natural frequencies of the cracked beams and it gives good results for shallow cracks. An extensive study has been made on diagnosis of fracture damage in structure [10]. The concept of fracture hinge has been developed analytically and the same has been applied to a cracked section for detecting fracture damage in simple structures. It has been verified experimentally that the structural effect of a cracked section can be represented by an equivalent spring loaded hinge.

The fuzzy finite element method for static analysis of engineering systems can be done by using an optimization-based scheme taking fuzzy parameters, geometry, and applied loads into consideration [11]. The mobile-robot navigation control system can be designed using fuzzy logic [12]. Fuzzy rules embedded in the controller of a mobile robot enable it to avoid obstacles in a cluttered environment that includes other mobile robots. A fuzzy finite element approach

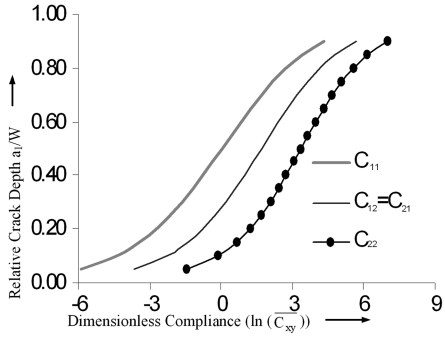


**Fig. 2 Relative crack depth $a_1/w$ vs dimensionless compliance $\ell n\, \bar{C}_{xy}$.**

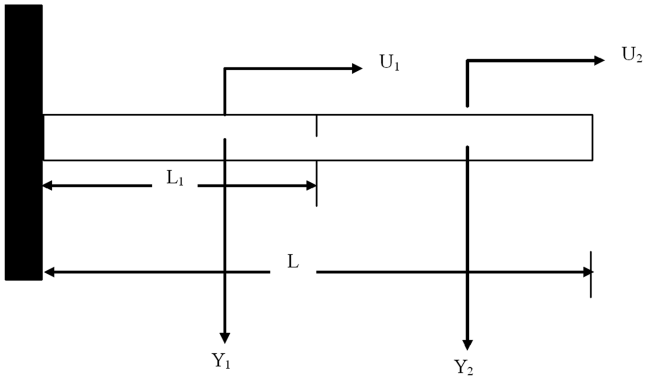


**Fig. 3 Beam model.**

can be used for modeling smart structures with vague or imprecise uncertainties [13]. A fuzzy finite element method can be applied for vibration analysis of imprecisely defined systems by using a search-based algorithm [14]. The approach enhances the computational efficiency in fuzzy operations for identifying the system dynamic responses. A fuzzy arithmetical approach can be used for the solution of finite element problems involving uncertain parameters [15].

In this paper, fault detection of the cracked beam using a fuzzy Gaussian inference system has been discussed. Fuzzy rules are outlined from the theoretical analysis for the fuzzy inference systems. The strain-energy release rate is used to find the influence of the crack on the local stiffness of the beam. Boundary conditions are outlined so that they can take the effect of the crack in calculation of the natural frequencies and mode shapes of the cracked beam. The

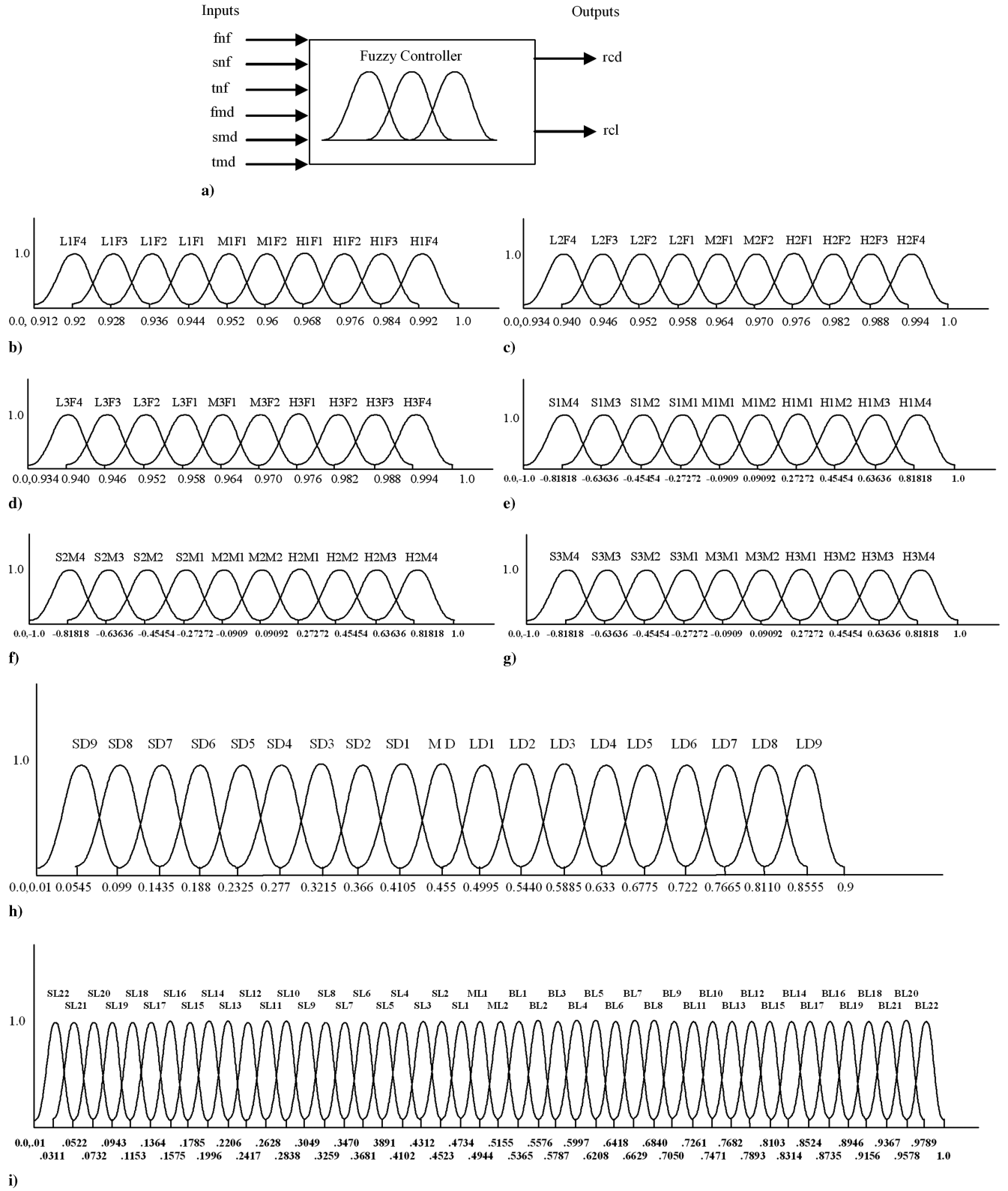


**Fig. 4 Illustrations of a) fuzzy controller; membership functions for the relative natural frequency for the b) first mode of vibration, c) second mode of vibration, and d) third mode of vibration; membership functions for the relative mode shape difference for the e) first mode of vibration, f) second mode of vibration, and g) third mode of vibration; and membership functions for the h) relative crack depth and i) relative crack location.**

fuzzy inference system developed consists of six input parameters and two output parameters. The input parameters are relative deviation of the first three natural frequencies and first three mode shapes. The output parameters of the fuzzy inference systems are relative crack depth and relative crack location.

## II. Theoretical Analysis

### A. Local Flexibility of a Cracked Beam Under Bending and Axial Loading

The presence of a transverse surface crack of depth $a_1$ on beam of width $B$ and height $W$ introduces a local flexibility that can be defined in matrix form, the dimension of which depends on the degrees of freedom. Here, a $2 \times 2$ matrix is considered. A cantilever beam is subjected to axial force $P_1$ and bending moment $P_2$, shown in Fig. 1a, which gives coupling with the longitudinal and transverse motion.

The strain-energy release rate at the fractured section can be written as [16] $J = (1/E')(K_{I1} + K_{I2})^2$, where $1/E' = (1 - v^2)/E'$ for the plane-strain condition and $1/E$ for the plane-stress condition.

$K_{I1}$, $K_{I2}$ are the stress-intensity factors of mode I (opening of the crack) for load $P_1$ and $P_2$, respectively. The values of stress-intensity factors from earlier studies [16] are

$$K_{I1} = \frac{P_1}{BW}\sqrt{\pi a}\left(F_1\left(\frac{a}{W}\right)\right), \qquad K_{I2} = \frac{6P_2}{BW^2}\sqrt{\pi a}\left(F_2\left(\frac{a}{W}\right)\right)$$

where expressions for $F_1$ and $F_2$ are as follows:

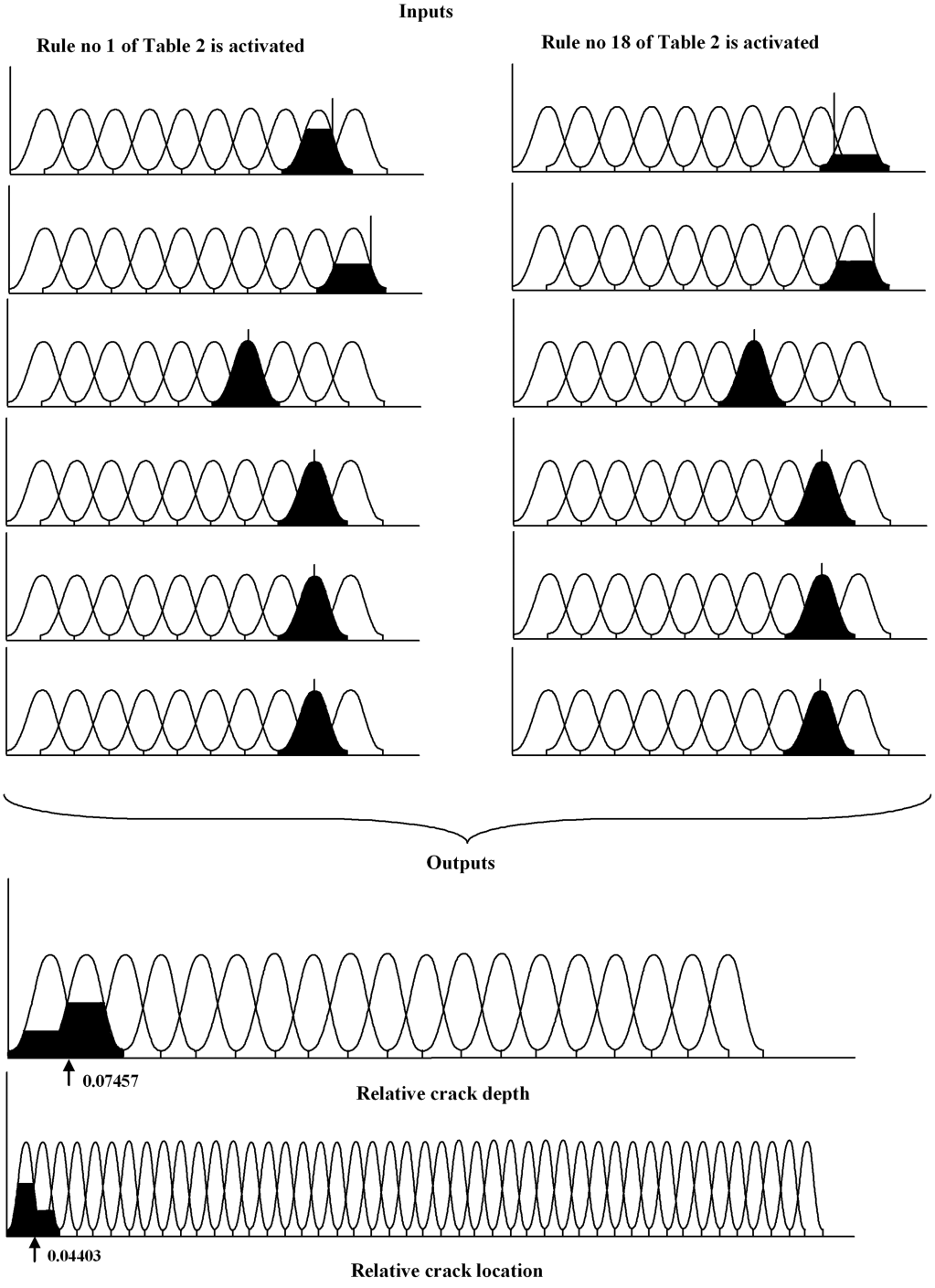


**Fig. 5 Resultant values of relative crack depth and relative crack location when rules 1 and 18 of Table 2 are activated.**

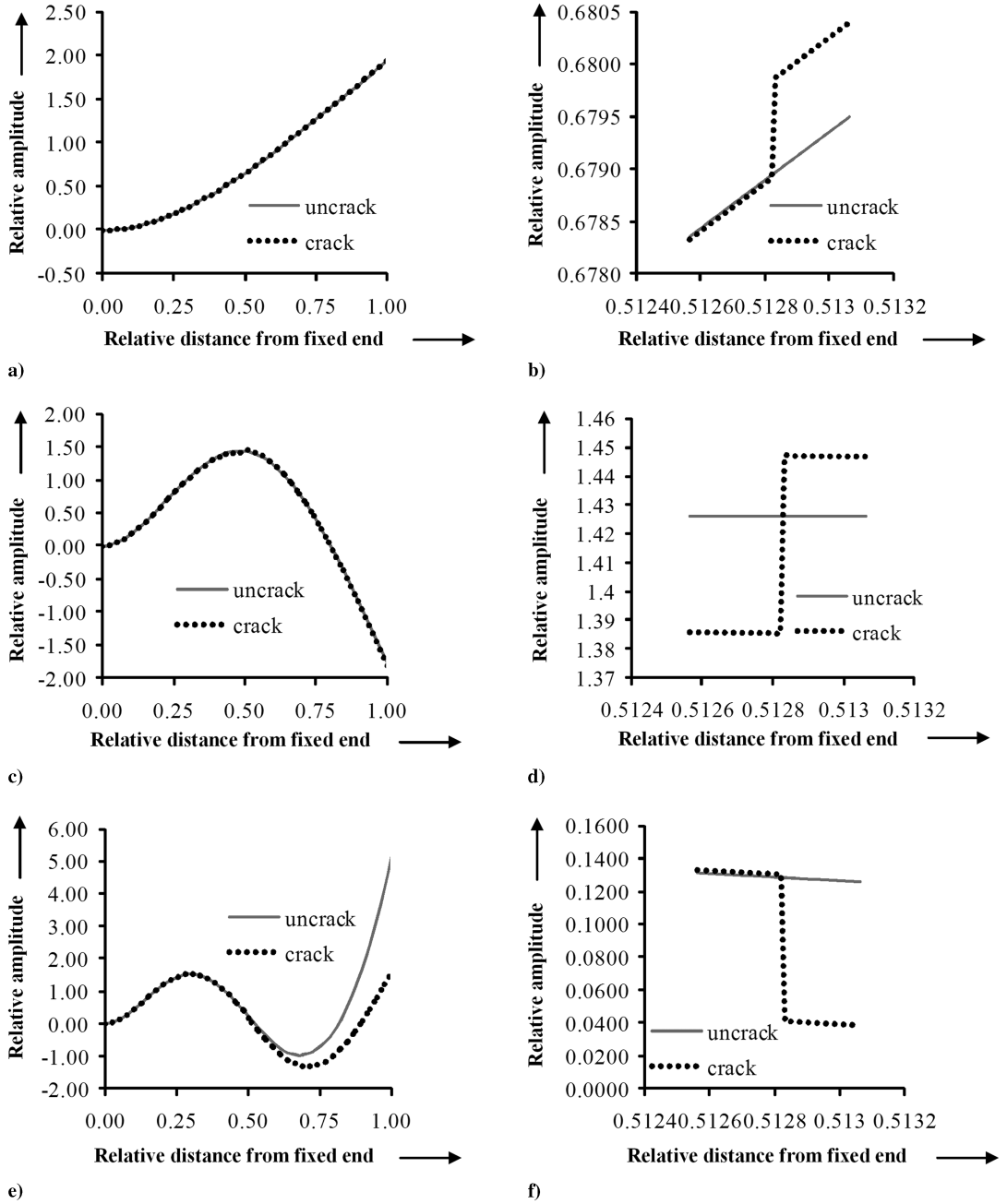


**Fig. 6 Relative amplitude vs relative distance from the fixed end at $a_1/W = 0.2$ and $L_1/L = 0.5128$ for a) first mode of vibration, b) magnified view of the first mode at the vicinity of the crack location, c) second mode of vibration, d) magnified view of the second mode at the vicinity of the crack location, e) third mode of vibration, and f) magnified view of the third mode at the vicinity of the crack location.**

$$F_1\left(\frac{a}{W}\right), \quad = \left(\frac{2W}{\pi a}\tan\left(\frac{\pi a}{2W}\right)\right)^{0.5} \times \left\{\frac{0.752 + 2.02(a/W) + 0.37(1 - \sin(\pi a/2W))^3}{\cos(\pi a/2W)}\right\}$$

$$F_2\left(\frac{a}{W}\right), \quad = \left(\frac{2W}{\pi a}\tan\left(\frac{\pi a}{2W}\right)\right)^{0.5} \times \left\{\frac{0.923 + 0.199(1 - \sin(\pi a/2W))^4}{\cos(\pi a/2W)}\right\}$$

Let $U_t$ be the strain energy due to the crack. Then from Castigliano's theorem, the additional displacement along the force $P_i$ is

$$u_i = \frac{\partial U_t}{\partial P_i} \tag{1}$$

The strain energy will have the form

$$U_t = \int_0^{a_1} \frac{\partial U_t}{\partial a}\mathrm{d}a = \int_0^{a_1} J\mathrm{d}a \tag{2}$$

where $J = \partial U_t/\partial a$ is the strain-energy density function.

From Eqs. (1) and (2), we thus have

$$u_i = \frac{\partial}{\partial P_i}\left[\int_0^{a_1} J(a)\mathrm{d}a\right] \tag{3}$$

The flexibility influence coefficient $C_{ij}$ will be, by definition,

$$C_{ij} = \frac{\partial u_i}{\partial P_j} = \frac{\partial^2}{\partial P_i \partial P_j} \int_0^{a_1} J(a)\mathrm{d}a \tag{4}$$

To find the final flexibility matrix, we have to integrate over the breadth $B$:

$$C_{ij} = \frac{\partial u_i}{\partial P_j} = \frac{\partial^2}{\partial P_i \partial P_j} \int_{-B/2}^{+B/2} \int_0^{a_1} J(a)\mathrm{d}a\mathrm{d}z \tag{5}$$

Adding the preceding value strain-energy release rate, Eq. (5) modifies as

$$C_{ij} = \frac{B}{E'} \frac{\partial^2}{\partial P_i \partial P_j} \int_0^{a_1} (K_{l1} + K_{l2})^2 \mathrm{d}a \tag{6}$$

Adding $\xi = (a/w)$ and $\mathrm{d}\xi = \mathrm{d}a/W$, we get $\mathrm{d}a = W\,\mathrm{d}\xi$, and when $a = 0$ and $\xi = 0$, then $a = a_1$ and $\xi = a_1/W = \xi_1$.

From the preceding condition, Eq. (6) converts to

$$C_{ij} = \frac{BW}{E'} \frac{\partial^2}{\partial P_i \partial P_j} \int_0^{\xi_1} (K_{l1} + K_{l2})^2 \mathrm{d}\xi \tag{7}$$

From Eq. (7), calculating $C_{11}$, $C_{12}$ $(=C_{21})$, and $C_{22}$, we get

$$C_{11} = \frac{BW}{E'} \int_0^{\xi_1} \frac{\pi a}{B^2 W^2} 2(F_1(\xi))^2 \mathrm{d}\xi = \frac{2\pi}{BE'} \int_0^{\xi_1} \xi (F_1(\xi))^2 \mathrm{d}\xi \tag{8}$$

$$C_{12} = C_{21} = \frac{12\pi}{E'BW} \int_0^{\xi_1} \xi F_1(\xi) F_2(\xi) \mathrm{d}\xi \tag{9}$$

$$C_{22} = \frac{72\pi}{E'BW^2} \int_0^{\xi_1} \xi F_2(\xi) F_2(\xi) \mathrm{d}\xi \tag{10}$$

Converting the influence coefficient into dimensionless form,

**Table 1 Description of fuzzy linguistic terms**

| Membership function names | Linguistic terms | Description and range of the linguistic terms |
|---|---|---|
| L1F1, L1F2, L1F3, L1F4 | $\mathrm{fnf}_{1\text{ to }4}$ | Low ranges of relative natural frequency for the first mode of vibration in descending order |
| M1F1, M1F2 | $\mathrm{fnf}_{5,6}$ | Medium ranges of relative natural frequency for the first mode of vibration in ascending order |
| H1F1, H1F2, H1F3, H1F4 | $\mathrm{fnf}_{7\text{ to }10}$ | Large ranges of relative natural frequency for the first mode of vibration in ascending order |
| L2F1, L2F2, L2F3, L2F4 | $\mathrm{snf}_{1\text{ to }4}$ | Low ranges of relative natural frequency for the second mode of vibration in descending order |
| M2F1, M2F2 | $\mathrm{snf}_{5,6}$ | Medium ranges of relative natural frequency for the second mode of vibration in ascending order |
| H2F1, H2F2, H2F3, H2F4 | $\mathrm{snf}_{7\text{ to }10}$ | Large ranges of relative natural frequencies for the second mode of vibration in ascending order |
| L3F1, L3F2, L3F3, L3F4 | $\mathrm{tnf}_{1\text{ to }4}$ | Low ranges of relative natural frequencies for the third mode of vibration in descending order |
| M3F1, M3F2 | $\mathrm{tnf}_{5,6}$ | Medium ranges of relative natural frequencies for the third mode of vibration in ascending order |
| H3F1, H3F2, H3F3, H3F4 | $\mathrm{tnf}_{7\text{ to }10}$ | Large ranges of relative natural frequencies for the third mode of vibration in ascending order |
| S1M1, S1M2, S1M3, S1M4 | $\mathrm{fmd}_{1\text{ to }4}$ | Small ranges of the first relative mode shape difference in descending order |
| M1M1, M1M2 | $\mathrm{fmd}_{5,6}$ | Medium ranges of the first relative mode shape difference in ascending order |
| H1M1, H1M2, H1M3, H1M4 | $\mathrm{fmd}_{7\text{ to }10}$ | Large ranges of the first relative mode shape difference in ascending order |
| S2M1, S2M2, S2M3, S2M4 | $\mathrm{smd}_{1\text{ to }4}$ | Small ranges of the second relative mode shape difference in descending order |
| M2M1, M2M2 | $\mathrm{smd}_{5,6}$ | Medium ranges of the second relative mode shape difference in ascending order |
| H2M1, H2M2, H2M3, H2M4 | $\mathrm{smd}_{7\text{ to }10}$ | Large ranges of the second relative mode shape difference in ascending order |
| S3M1, S3M2, S3M3, S3M4 | $\mathrm{tmd}_{1\text{ to }4}$ | Small ranges of the third relative mode shape difference in descending order |
| M3M1, M3M2 | $\mathrm{tmd}_{5,6}$ | Medium ranges of the third relative mode shape difference in ascending order |
| H3M1, H3M2, H3M3, H3M4 | $\mathrm{tmd}_{7\text{ to }10}$ | Large ranges of the third relative mode shape difference in ascending order |
| SL1, SL2,. . .,SL22 | $\mathrm{rcl}_{1\text{ to }22}$ | Small ranges of relative crack location in descending order |
| ML1, ML2 | $\mathrm{rcl}_{23,24}$ | Medium ranges of relative crack location in ascending order |
| BL1, BL2,. . .,BL22 | $\mathrm{rcl}_{25\text{ to }46}$ | Large ranges of relative crack location in ascending order |
| SD1, SD2,. . .,SD9 | $\mathrm{rcd}_{1\text{ to }9}$ | Small ranges of relative crack depth in descending order |
| MD | $\mathrm{rcd}_{10}$ | Medium relative crack depth |
| LD1, LD2,. . .,LD9 | $\mathrm{rcd}_{11\text{ to }19}$ | Large ranges of relative crack depth in ascending order |

**Table 2 Examples of 20 fuzzy rules used in fuzzy controller**

| Serial no. | Examples of some rules used in the fuzzy controller |
|---|---|
| 1 | If fnf is H1F3, snf is H2F4, tnf is H3F1, fmd is H1M3, smd is H2M3, tmd is H3M3, then rcd is SD8, and rcl is SL22 |
| 2 | If fnf is H1F3, snf is H2F3, tnf is H3F1, fmd is H1M3, smd is H2M3,tmd is H3M3, then rcd is SD8, and rcl is SL22 |
| 3 | If fnf is H1F1, snf is M2F1, tnf is L3F2, fmd is H1M4, smd is H2M4, tmd is H3M4, then rcd is MD, and rcl is SL22 |
| 4 | If fnf is M1F1, snf is L2F2, tnf is L3F2, fmd is H1M4, smd is H2M4, tmd is H3M4, then rcd is LD5, and rcl is SL22 |
| 5 | If fnf is H1F1, snf is M2F1, tnf is L3F1, fmd is H1M3, smd is H2M3, tmd is H3M3, then rcd is LD1, and rcl is SL21 |
| 6 | If fnf is M1F1, snf is L2F1, tnf is L3F2, fmd is H1M4, smd is H2M3, tmd is H3M4, then rcd is LD6, and rcl is SL21 |
| 7 | If fnf is H1F2, snf is M2F2, tnf is M3F2, fmd is H1M3, smd is H2M3, tmd is H3M9, then rcd is SD1, and rcl is SL20 |
| 8 | If fnf is H1F3, snf is H2F4, tnf is H3F2, fmd is H1M2, smd is H2M1, tmd is H3M2, then rcd is SD7, and rcl is SL19 |
| 9 | If fnf is H1F1, snf is M2F2, tnf is H3F2, fmd is H1M2, smd is H2M2, tmd is H3M2, then rcd is LD2, and rcl is SL18 |
| 10 | If fnf is H1F3, snf is H2F4, tnf is H3F3, fmd is S1M1, smd is S2M1, tmd is S3M1, then rcd is SD3, and rcl is SL17 |
| 11 | If fnf is H1F1, snf is H2F3, tnf is H3F2, fmd is H1M2, smd is H2M1, tmd is H3M1, then rcd is LD2, and rcl is SL16 |
| 12 | If fnf is H1F2, snf is H2F4, tnf is H3F2, fmd is H1M2, smd is M2M2, tmd is H3M2, then rcd is LD1, and rcl is SL15 |
| 13 | If fnf is H1F2, snf is H2F4, tnf is H3F1, fmd is H1M2, smd is M2M2, tmd is H3M2, then rcd is MD, and rcl is SL14 |
| 14 | If fnf is M1F2, snf is M2F1,tnf is L3F3, fmd is H1M2, smd is H2M2, tmd is H3M3, then rcd is LD9, and rcl is SL7 |
| 15 | If fnf is H1F1, snf is H2F4, tnf is M3F1, fmd is H1M2, smd is M2M2, tmd is H3M3, then rcd is LD4, and rcl is SL13 |
| 16 | If fnf is H1F3, snf is H2F4, tnf is M3F1, fmd is H1M2, smd is H2M1, tmd is H3M3, then rcd is SD2, and rcl is SL10 |
| 17 | If fnf is M1F1, snf is M2F2, tnf is L3F3,fmd is H1M2,smd is H2M2,tmd is H3M3, then rcd is LD9,and rcl is SL9 |
| 18 | If fnf is H1F4, snf is H2F4, tnf is H3F1, fmd is H1M3, smd is H2M3, tmd is H3M3, then rcd is SD9, and rcl is SL21 |
| 19 | If fnf is H1F2, snf is H2F4, tnf is L3F1, fmd is H1M2, smd is M2M1, tmd is H3M3, then rcd is LD3, and rcl is SL12 |
| 20 | If fnf is H1F4, snf is H2F3, tnf is M3F2, fmd is M1M1, smd is H2M2, tmd is H3M3, then rcd is SD4, and rcl is BL7 |

$$\bar{C}_{11} = C_{11}\frac{BE'}{2\pi}\bar{C}_{12} = C_{12}\frac{E'BW}{12\pi} = \bar{C}_{21}; \bar{C}_{22} = C_{22}\frac{E'BW^2}{72\pi}$$

The local stiffness matrix can be obtained by taking the inversion of compliance matrix; that is,

$$K = \begin{bmatrix} K_{11} & K_{12} \\ K_{21} & K_{22} \end{bmatrix} = \begin{bmatrix} C_{11} & C_{12} \\ C_{21} & C_{22} \end{bmatrix}^{-1}$$

Figure 2 shows the variation of dimensionless compliances to that of the relative crack depth.

### B. Analysis of Vibration Characteristics of the Cracked Beam

*1. Free Vibration*

A cantilever beam of length $L$, width $B$, and depth $W$ with a crack of depth $a_1$ at a distance $L_1$ from the fixed end is considered shown in Fig. 1. Taking $u_1(x, t)$ and $u_2(x, t)$ as the amplitudes of longitudinal vibration for the sections before and after the crack, then $y_1(x, t)$ and $y_2(x, t)$ are the amplitudes of bending vibration for the same sections shown in Fig. 3.

The normal function for the system can be defined as

$$\bar{u}_1(\bar{x}) = A_1\cos(\bar{K}_u\bar{x}) + A_2\sin(\bar{K}_u\bar{x}) \tag{11a}$$

$$\bar{u}_2(\bar{x}) = A_3\cos(\bar{K}_u\bar{x}) + A_4\sin(\bar{K}_u\bar{x}) \tag{11b}$$

$$\bar{y}_1(\bar{x}) = A_5\cosh(\bar{K}_y\bar{x}) + A_6\sinh(\bar{K}_y\bar{x}) + A_7\cos(\bar{K}_y\bar{x}) + A_8\sin(\bar{K}_y\bar{x}) \tag{11c}$$

$$\bar{y}_2(\bar{x}) = A_9\cosh(\bar{K}_y\bar{x}) + A_{10}\sinh(\bar{K}_y\bar{x}) + A_{11}\cos(\bar{K}_y\bar{x}) + A_{12}\sin(\bar{K}_y\bar{x}) \tag{11d}$$

where

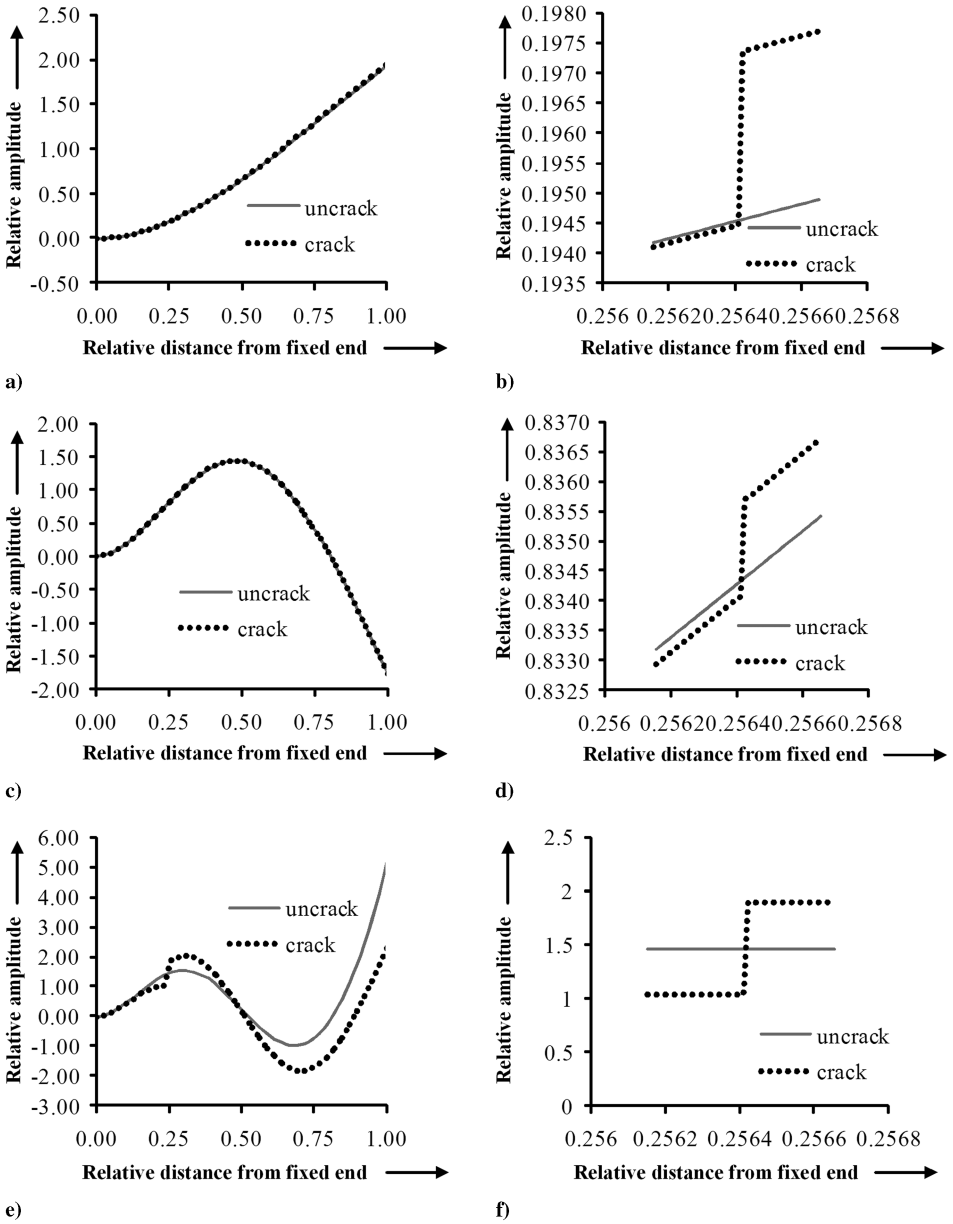


**Fig. 7 Relative amplitude vs relative distance from the fixed end at $a_1/W = 0.3$ and $L_1/L = 0.2564$ for a) first mode of vibration, b) magnified view of the first mode at the vicinity of the crack location, c) second mode of vibration, d) magnified view of the second mode at the vicinity of the crack location, e) third mode of vibration, f) magnified view of the third mode at the vicinity of the crack location.**

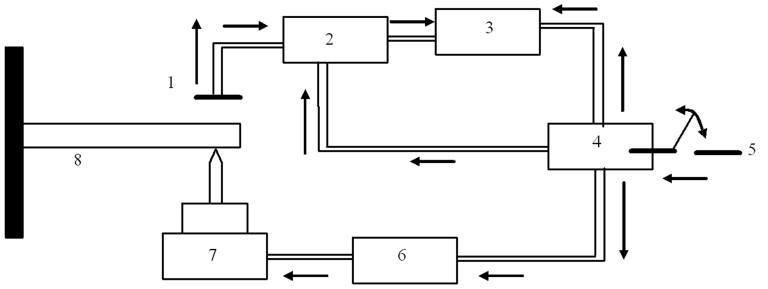


1. Vibration Pick-up
2. Amplifier
3. Vibration indicator
4. Distribution box
5. Power supply
6. Power amplifier
7. Vibration generator
8. Cantilever beam

**Fig. 8 Schematic block diagram of experimental setup.**

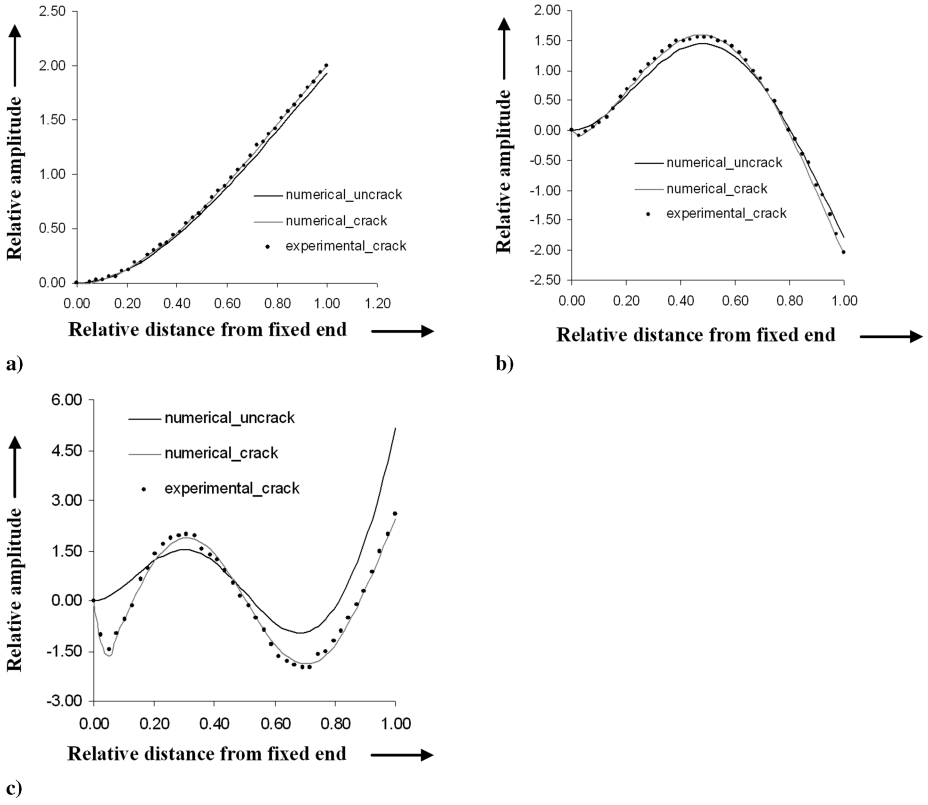


**Fig. 9 Relative amplitude vs relative distance from the fixed end at $a_1/W = 0.4$ and $L_1/L = 0.026$ for the a) first mode of vibration, b) second mode of vibration, and c) third mode of vibration.**

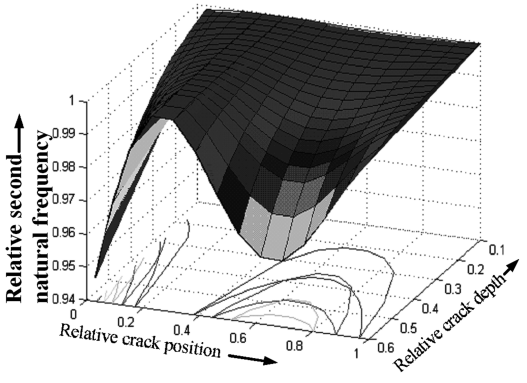


**Fig. 10 Three-dimensional and contour plots for relative natural frequency.**

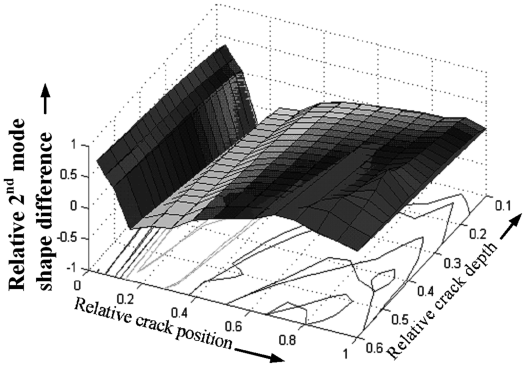


**Fig. 11 Three-dimensional and contour plots for relative mode shape difference.**

$$\bar{x}=\frac{x}{L},\qquad \bar{u}=\frac{u}{L},\qquad \bar{y}=\frac{y}{L},\qquad \beta=\frac{L_1}{L}$$
$$\bar{K}_u=\frac{\omega L}{C_u},\qquad C_u=\left(\frac{E}{\rho}\right)^{1/2},\qquad \bar{K}_y=\left(\frac{\omega L^2}{C_y}\right)^{1/2}$$
$$C_y=\left(\frac{EI}{\mu}\right)^{1/2},\qquad \mu=A\rho$$

where $A_i$ ($i=1$ to 12) are constants are to be determined from boundary conditions. The boundary conditions of the cantilever beam in consideration are

$$\bar{u}_1(0)=0,\qquad \bar{y}_1(0)=0,\qquad \bar{y}_1'(0)=0$$
$$\bar{u}_2'(1)=0,\qquad \bar{y}_2''(1)=0,\qquad \bar{y}_2'''(1)=0$$

At the cracked section,

$$\bar{u}_1(\beta)=\bar{u}_2(\beta),\qquad \bar{y}_1(\beta)=\bar{y}_2(\beta)$$
$$\bar{y}_1''(\beta)=\bar{y}_2''(\beta),\qquad \bar{y}_1'''(\beta)=\bar{y}_2'''(\beta)$$

Also at the cracked section, we have

$$AE\frac{\mathrm{d}u_1(L_1)}{\mathrm{d}x}=K_{11}(u_2(L_1)-u_1(L_1))+K_{12}\left(\frac{\mathrm{d}y_2(L_1)}{\mathrm{d}x}-\frac{\mathrm{d}y_1(L_1)}{\mathrm{d}x}\right)$$

Multiplying both sides of the preceding equation by $AE/LK_{11}K_{12}$, we get

$$M_1M_2\bar{u}'(\beta)=M_2(\bar{u}_2(\beta)-\bar{u}_1(\beta))+M_1(\bar{y}_2'(\beta)-\bar{y}_1'(\beta))$$

Similarly,

$$EI\frac{\mathrm{d}^2y_1(L_1)}{\mathrm{d}x^2}=K_{21}(u_2(L_1)-u_1(L_1))+K_{22}(\frac{\mathrm{d}y_2(L_1)}{\mathrm{d}x}-\frac{\mathrm{d}y_1(L_1)}{\mathrm{d}x})$$

Multiplying both sides of the preceding equation by $EI/L^2K_{22}K_{21}$, we get

$$M_3M_4\bar{y}_1''(\beta)=M_3(\bar{u}_2(\beta)-\bar{u}_1(\beta))+M_4(\bar{y}_2'(\beta)-\bar{y}_1'(\beta))$$

where

$$M_1=\frac{AE}{LK_{11}},\qquad M_2=\frac{AE}{K_{12}},\qquad M_3=\frac{EI}{LK_{22}},\qquad M_4=\frac{EI}{L^2K_{21}}$$

The normal functions, Eq. (11), and the preceding boundary conditions yield the characteristic equation of the system as

$$|Q|=0 \tag{12}$$

This determinant is a function of natural circular frequency $\omega$, the relative location of the crack $\beta$, and the local stiffness matrix $K$, which is in turn a function of the relative crack depth $a_1/W$.

*2. Forced Vibration*

If the cantilever beam with a transverse crack is excited at its free end by a harmonic excitation [$Y=Y_0\sin(\omega t)$], the nondimensional amplitude at the free end may be expressed as $\bar{y}_2(1)=y_0/L=\bar{y}_0$. Therefore, the boundary conditions for the beam remain the same as before, except for the boundary condition $\bar{y}_2'''(1)=0$, which is modified as $\bar{y}_2(1)=\bar{y}_0$.

The constants $A_i$ ($i=1$ to 12) are then computed from the algebraic condition:

$$Q_1D=B_1 \tag{13}$$

where $Q_1$ is the $12\times 12$ matrix obtained from the preceding boundary conditions, $D$ is a column matrix obtained from the constants, and $B_1$ is a column matrix, the transpose of which is given by

$$B_1^T=[0\quad 0\quad 0\quad \bar{y}_0\quad 0\quad 0\quad 0\quad 0\quad 0\quad 0\quad 0\quad 0]$$

## III. Analysis of the Fuzzy Controller

The fuzzy controller developed has six input parameters and two output parameters. The linguistic terms used for the inputs are as follows: relative first natural frequency (fnf), relative second natural frequency (snf), relative third natural frequency (tnf), relative first mode shape difference (fmd), relative second mode shape difference (smd), and relative third mode shape difference (tmd). The linguistic terms used for the outputs are as follows: relative crack location (rcl) and relative crack depth (rcd).

The fuzzy controller used in the present paper is shown in Fig. 4a. The Gaussian membership functions are shown pictorially in Figs. 4b–4i. The linguistic terms for the Gaussian membership functions used in the fuzzy controller are described in Table 1.

### A. Fuzzy Mechanism for Crack Detection

Based on the preceding fuzzy subsets, the fuzzy control rules are defined in a general form as follows:

$$\text{If}\ \ (\text{fnf is fnf}_i\,\Lambda\,\text{snf is snf}_j\,\Lambda\,\text{tnf is tnf}_k\,\Lambda\,\text{fmd is fmd}_l\,\Lambda\,\text{smd is smd}_m\,\Lambda\,\text{tmd is tmd}_n)\quad \text{then rcl is rcl}_{ijklmn}\,\Lambda\,\text{rcd is rcd}_{ijklmn} \tag{14}$$

where

$$i=1\text{ to }10,\qquad j=1\text{ to }10,\qquad k=1\text{ to }10,\qquad l=1\text{ to }10\qquad m=1\text{ to }10,\qquad n=1\text{ to }10$$

because fnf, snf, tnf, fmd, smd, and tmd have ten membership functions each.

From expression (14), two set of rules can be written:

$$\begin{aligned}&\text{If}\ \ (\text{fnf is fnf}_i\,\Lambda\,\text{snf is snf}_j\,\Lambda\,\text{tnf is tnf}_k\,\Lambda\,\text{fmd is fmd}_l\,\Lambda\,\text{smd is smd}_m\,\Lambda\,\text{tmd is tmd}_n)\quad \text{then rcl is rcl}_{ijklmn}\\&\text{If}\ \ (\text{fnf is fnf}_i\,\Lambda\,\text{snf is snf}_j\,\Lambda\,\text{tnf is tnf}_k\,\Lambda\,\text{fmd is fmd}_l\,\Lambda\,\text{smd is smd}_m\,\Lambda\,\text{tmd is tmd}_n)\quad \text{then rcd is rcd}_{ijklmn}\end{aligned} \tag{15}$$

According to the usual fuzzy-logic control method [12], a factor $W_{ijklmn}$ is defined for the rules as follows:

$$W_{ijklmn}=\mu_{\text{fnf}_i}(\text{freq}_i)\,\Lambda\,\mu_{\text{snf}_j}(\text{freq}_j)\,\Lambda\,\mu_{\text{tnf}_k}(\text{freq}_k)\,\Lambda\,\mu_{\text{fmd}_l}\times(\text{moddif}_l)\,\Lambda\,\mu_{\text{smd}_m}(\text{moddif}_m)\,\Lambda\,\mu_{\text{tmd}_n}(\text{moddif}_n)$$

**Table 3 Comparison of results between fuzzy controller, numerical analysis and experimental setup**

| | | | | | | Fuzzy controller | | Numerical | | Experimental | |
|---|---|---|---|---|---|---|---|---|---|---|---|
| Relative fnf | Relative snf | Relative tnf | Relative fmd | Relative smd | Relative tmd | rcd | rcl | rcd | rcl | rcd | rcl |
| 0.9848 | 0.9958 | 0.9975 | 0.2709 | 0.2372 | 0.3158 | 0.203 | 5.71 | 0.202 | 5.51 | 0.205 | 5.8 |
| 0.9673 | 0.9874 | 0.9943 | 0.3969 | 0.3247 | 0.3923 | 0.431 | 6.51 | 0.427 | 6.32 | 0.43 | 6.71 |
| 0.9623 | 0.9948 | 0.9983 | 0.1814 | 0.0279 | 0.0774 | 0.548 | 12.73 | 0.537 | 12.79 | 0.568 | 12.6 |
| 0.9756 | 0.9976 | 0.9972 | 0.1383 | −0.0823 | 0.1898 | 0.389 | 14.98 | 0.394 | 14.94 | 0.391 | 15.02 |
| 0.9852 | 0.9984 | 0.9967 | 0.01 | −0.8678 | 0.2572 | 0.227 | 18.95 | 0.231 | 18.9 | 0.23 | 19.2 |
| 0.9723 | 0.9961 | 0.9818 | 0.1947 | 0.0672 | 0.4105 | 0.552 | 22.7 | 0.556 | 22.6 | 0.545 | 22.9 |
| 0.9823 | 0.9872 | 0.9919 | 0.0726 | 0.2567 | 0.3994 | 0.449 | 32.35 | 0.451 | 32.31 | 0.447 | 32.41 |
| 0.981 | 0.9809 | 0.9931 | 0.0898 | 0.3154 | 0.392 | 0.495 | 33.89 | 0.497 | 33.91 | 0.495 | 33.88 |
| 0.986 | 0.9842 | 0.9988 | −0.032 | 0.322 | 0.3965 | 0.425 | 40.15 | 0.426 | 40.1 | 0.425 | 40.3 |
| 0.9834 | 0.9685 | 0.9974 | 0.038 | 0.4558 | 0.3507 | 0.537 | 42.65 | 0.542 | 42.8 | 0.535 | 42.65 |

where $\text{freq}_i$, $\text{freq}_j$, and $\text{freq}_k$ are the first, second, and third relative natural frequencies of the cantilever beam with a crack, respectively; $\text{moddif}_l$, $\text{moddif}_m$, and $\text{moddif}_n$ are the first, second, and third relative mode shape differences of the cantilever beam with crack, respectively. By applying the composition rule of inference [12], the membership values of the relative crack location and relative crack depth, $(\text{location})_{\text{rcl}}$ and $(\text{depth})_{\text{rcd}}$, can be computed as

$$\left.\begin{aligned}\mu_{\text{rcl}_{ijklmn}}(\text{location}) &= W_{ijklmn} \Lambda \mu_{\text{rcl}_{ijklmn}}(\text{location}) \qquad \forall_{\text{length}} \in \text{rcl}\\ \mu_{\text{rcd}_{ijklmn}}(\text{depth}) &= W_{ijklmn} \Lambda \mu_{\text{rcd}_{ijklmn}}(\text{depth}) \qquad \forall_{\text{depth}} \in \text{rcd}\end{aligned}\right\} \tag{16}$$

The overall conclusion by combining the outputs of all the fuzzy rules can be written as follows:

$$\left.\begin{aligned}\mu_{\text{rcl}}(\text{location}) &= \mu_{\text{rcl}_{111111}}(\text{location}) \vee, \ldots, \vee \mu_{\text{rcl}_{ijklmn}}(\text{location}) \vee, \ldots,\\ &\quad \times \vee \mu_{\text{rcl}_{10\ 10\ 10\ 10\ 10\ 10}}(\text{location})\\ \mu_{\text{rcd}}(\text{depth}) &= \mu_{\text{rcd}_{111111}}(\text{depth}) \vee, \ldots, \vee \mu_{\text{rcd}_{ijklmn}}(\text{depth}) \vee, \ldots,\\ &\quad \times \vee \mu_{\text{rcd}_{10\ 10\ 10\ 10\ 10\ 10}}(\text{depth})\end{aligned}\right\} \tag{17}$$

The crisp values of rcl and rcd are computed using the center-of-gravity method [12] as

$$\left.\begin{aligned}\text{rcl} &= \frac{\int(\text{location}) \cdot \mu_{\text{rcl}}(\text{location}) \cdot d(\text{location})}{\int \mu_{\text{rcl}}(\text{location}) \cdot d(\text{location})}\\ \text{rcd} &= \frac{\int(\text{depth}) \cdot \mu_{\text{rcd}}(\text{depth}) \cdot d(\text{depth})}{\int \mu_{\text{rcd}}(\text{depth}) \cdot d(\text{depth})}\end{aligned}\right\} \tag{18}$$

### B. Fuzzy Controller for Finding Crack Depth and Crack Location

The inputs to the fuzzy controller are fnf, snf, tnf, fmd, smd, and tmd. The outputs from the fuzzy controller are rcd and rcl. Twenty of the several hundred fuzzy rules are listed in Table 2. Figure 5 shows the fuzzy controller results when rule 1 and rule 18 are activated from Table 2.

## IV. Experimental Setup

An experimental setup used for performing the experiments is shown in the schematic diagram in Fig. 8. A number of tests are conducted on an aluminium beam specimen ($800 \times 50 \times 6$ mm) with a transverse crack for determining the natural frequencies and mode shapes for different crack depths. Experimental results of amplitude of transverse vibration at various locations along the length of the beam are recorded by positioning the vibration pickup and tuning the vibration generator at the corresponding resonant frequencies. The results for the first three modes are plotted in Fig. 9. Corresponding numerical results are also presented in the same graph for comparison.

## V. Discussion

From the predicted results of developed fuzzy Gaussian inference technique, numerical, and experimental analyses, the following points are drawn. It is evident from the Fig. 2 that as the relative crack depth increases, the compliances $C_{11}$, $C_{12} = C_{21}$, and $C_{22}$ increase. The linguistic forms of fuzzy rules for the fuzzy controller developed are listed in Table 1. Some examples of actual fuzzy rules formulated for the fuzzy controller are shown in Table 2. The Gaussian membership functions used for the fuzzy controller are depicted pictorially in Fig. 4. The results of the developed fuzzy Gaussian controller by activation of rule 1 and rule 18 from Table 2 are shown in Fig. 5. For different relative crack locations (0. 5128 and 0.2564) and relative crack depths (0.2 and 0.3), the first three mode shapes and their magnified views are drawn pictorially in Figs. 6 and 7. It is observed from Figs. 6 and 7 that there are reasonable changes in mode shapes when compared between the cracked and uncracked beams. The experimental and numerical results and their comparisons between the cracked and uncracked beams are represented graphically in Fig. 9. Figures 10 and 11, respectively, represent the variation of relative natural frequencies and relative mode shapes in three-dimensional forms, along with a contour plot with respect to the relative crack location and relative crack depth. Table 3 contains some of the predicted results by the developed fuzzy controller and their comparison with corresponding numerical and experimental results, which show very good agreement.

## VI. Conclusions

The following conclusions can be drawn on the basis of the results and discussions made from the present investigations. Because of the presence of a crack, the beam structure undergoes changes in natural frequencies and mode shapes. These changes depend upon the crack location and its intensity. The fuzzy controller considered here uses Gaussian membership functions and is used to predict the crack location and its intensity by using the relative crack location and relative crack depth as inputs. The fuzzy-controller-predicted results are reasonably acceptable and in agreement with the experimental data. The successful detection of the crack and its intensity in a cantilever beam demonstrates that the new technique developed in the present study can be used efficiently and effectively in crack identification in different beam-type structures. This developed fuzzy controller can be used as a smart fault-detecting tool for different types of vibrating structures. Further research can be made to generate a hybrid fuzzy controller for more efficient fault identification.

## References

[1] Wang, J., and Qiao, P., "Improved Damage Detection for Beam-Type Structures Using a Uniform Load Surface," *Structural Health Monitoring*, Vol. 6, No. 2, 2007, pp. 99–110. doi:10.1177/1475921706072062

[2] Karthikeyan, M. A., Tiwari, R. A., and Talukdar, S. B., "Crack Localization and Sizing in a Beam Based on the Free and Forced Response Measurement," *Mechanical Systems and Signal Processing*, Vol. 21, No. 3, 2007, pp. 1362–1385. doi:10.1016/j.ymssp.2006.06.002

[3] Wang, Z. H., Zhao, Y. G., and Ma, H. W., "Investigation on Crack Identification in the Beam-Type Structures," *Chinese Journal of Computational Mechanics*, Vol. 23, No. 3, 2006, pp. 307–312.
[4] Fabrizio, V., and Danilo, C., "Damage Detection in Beam Structures Based on Frequency Measurements," *Journal of Engineering Mechanics*, Vol. 126, No. 7, 2000, pp. 761–768. doi:10.1061/(ASCE)0733-9399(2000)126:7(761)
[5] Narkis, Y., "Identification of the Crack Location in Vibrating Simply Supported Beams," *Journal of Sound and Vibration*, Vol. 172, No. 4, 1994, pp. 549–558. doi:10.1006/jsvi.1994.1195
[6] Nian, G. S., Lin, Z. J., Sheng, J. J., and An, H. C., "A Vibration Diagnosis Approach to Structural Fault," *Journal of Vibration, Acoustics, Stress, and Reliability in Design*, Vol. 3, Jan. 1989, pp. 88–93.
[7] Behzad, M., Meghdari, A., and Ebrahimi, A. A., "Continuous Model for Forced Vibration Analysis of a Cracked Beam," American Society of Mechanical Engineers, Dynamic Systems and Control Div., Rept. DSC 74 DSC (2 ART B), New York, 2005, pp. 1849–1855.
[8] Behzad, M., Meghdari, A., and Ebrahimi, A., "A New Approach for Vibration Analysis of a Cracked Beam," *International Journal of Engineering. Transactions B, Applications*, Vol. 18, No. 4, 2005, pp. 319–330.
[9] Loya, J. A., Rubio, L., and Fernández-Sáez, J., "Natural Frequencies for Bending Vibrations of Timoshenko Cracked Beams," *Journal of Sound and Vibration*, Vol. 290, Nos. 3–5, 2006, pp. 640–653. doi:10.1016/j.jsv.2005.04.005
[10] Akgun, M., Ju, F. D., and Pacz, T. L., "Fracture Diagnosis in Beam Frame Structures Using Circuit Analogy," *Recent Advances in Engineering Mechanics and Their Impact on Civil Engineering Practice*, Vol. 2, ASCE Publications, Reston, VA, 1983, pp. 767–769.
[11] Rao, S. S., and Sawyer, J. P., "A Fuzzy Element Approach for the Analysis of Imprecisely-Defined System," *AIAA Journal*, Vol. 33, No. 12, 1995, pp. 2364–2370. doi:10.2514/3.12910
[12] Parhi, D. R., "Navigation of Mobile Robot Using a Fuzzy-Logic Controller," *Journal of Intelligent and Robotic Systems: Theory and Applications*, Vol. 42, No. 3, 2005, pp. 253–273. doi:10.1007/s10846-004-7195-x
[13] Akpan, U. O., Koko, T. S., Orisamolu, I. R., and Gallant, B. K., "Fuzzy Finite-Element Analysis of Smart Structures," *Smart Materials and Structures*, Vol. 10, No. 2, 2001, pp. 273–284. doi:10.1088/0964-1726/10/2/312
[14] Chen, L., and Rao, S. S., "Fuzzy Finite-Element Approach for the Vibration Analysis of Imprecisely-Defined Systems," *Finite Elements in Analysis and Design*, Vol. 27, No. 1, 1997, pp. 69–83. doi:10.1016/S0168-874X(97)00005-X
[15] Hanss, M., and Willner, K., "A Fuzzy Arithmetical Approach to the Solution of Finite Element Problems with Uncertain Parameters," *Mechanics Research Communications*, Vol. 27, No. 3, 2000, pp. 257–272. doi:10.1016/S0093-6413(00)00091-4
[16] Tada, H., Paris, P. C., and Irwin, G. R., *The Stress Analysis of the Cracks Hand Book*, Del Research Corp. Hellertown, PA, 1973.

A. Roy
*Associate Editor*